Third Order Nonlinear Optical Properties of Stacked Bacteriochlorophylls in Bacterial Photosynthetic Light-harvesting Proteins

L. X. Chen[a], Philip D. Laible[a], Frank C. Spano[b], Eric S. Manas[b]

[a]Chemistry Division, Argonne National Laboratory, Argonne, Illinois 60439
[b]Department of Chemistry, Temple University, Philadelphia, Pennsylvania 19122

CONF-970706--

ABSTRACT

Enhancement of the nonresonant second order molecular hyperpolarizabilities γ were observed in stacked macrocyclic molecular systems, previously in a μ-oxo silicon phthalocyanine (SiPcO) monomer, dimer and trimer series, and now in bacteriochlorophyll a (BChl$a$) arrays of light harvesting (LH) proteins. Compared to monomeric BChl$a$ in a tetrahydrofuran (THF) solution, the $<\gamma>$ for each macrocycle was enhanced in naturally occurring stacked macrocyclic molecular systems in the bacterial photosynthetic LH proteins where BChl$a$'s are arranged in tilted face-to-face arrays. In addition, the γ enhancement is more significant in B875 of LH1 than in B850 in LH2. Theoretical modeling of the nonresonant γ enhancement using simplified molecular orbitals for model SiPcO indicated that the energy level of the two photon state is crucial to the γ enhancement when a two photon process is involved, whereas the charge transfer between the monomers is largely responsible when one photon near resonant process is involved. The calculated results can be extended to γ enhancement in B875 and B850 arrays, suggesting that BChl$a$ in B875 are more strongly coupled than in B850. In addition, a 50-160 fold increase in $<\gamma>$ for the S_1 excited state of relative to S_0 of bacteriochlorophyll *in vivo* was observed which provides an alternative method for probing excited state dynamics and a potential application for molecular switching.

Key words: phthalocyanine, bacteriochlorophyll, light harvesting protein, third order nonlinear optical response, degenerate four wave mixing

1. INTRODUCTION

The enhancement of the third order nonlinear optical susceptibility $\chi^{(3)}$ as a function of number of π electrons in a linear or a planar molecule has been observed and can be explained as a result of conjugated π-electron delocalization on the same plane[1-3]. However, the effect of π-π electron interactions between different π-conjugated structures on $\chi^{(3)}$ is not well understood. Such a π-π electron interaction differs from the cases of in-plane one- and two-dimensional conjugated systems because the π-π electrons do not have direct covalent bonding and the π-π interaction occurs in a direction that is perpendicular to the π-electron conjugation plane. This kind of interaction often results from stacking π-conjugated molecules, such as organic crystals of π-conjugated systems, ordered liquid crystals of macrocycles, Langmuir-Blogett films, and BChl$a$ in bacterial photosynthetic reaction centers and light harvesting proteins.

We have previously measured the second hyperpolarizabilities $<\gamma>$ of a perfect "face-to-face" stacked macrocycle system, μ-oxo silicon phthalocyanine (SiPcO)$_n$ (n=1-3) using nonresonant degenerate four wave mixing (DFWM) at 1064 nm[4]. According to our results, $<\gamma>$ value for each monomer in this system is greatly enhanced as the number of monomer units in the oligomer increases[4]. We now extend our study to naturally occurring "face-to-face" macrocycle aggregates, BChl$a$ arrays in bacterial light
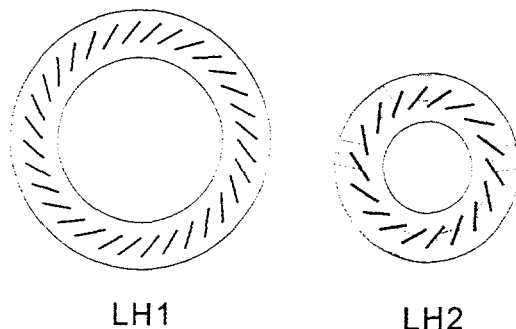

Figure 1 Graphic representations of the arrangement of BChl$a$ pigments in LH proteins based on known or proposed structures for the membrane-bound, pigment-protein complexes [6,7].

LH1   LH2

DISCLAIMER

DISCLAIMER

Portions of this document may be illegible in electronic image products. Images are produced from the best available original document.

harvesting complexes LH1 and LH2. The $<\gamma>$ values for each BChl$a$ unit in monomeric BChl$a$ solution, in LH1 and LH2 arrays are investigated. We also carried out a semi-empirical γ calculation on the "face-to-face" (SiPcO)$_n$ system, reproducing the trend of the $<\gamma>$ as a function of monomer numbers in the system[5]. The purpose of this study is to correlate the third order nonlinear optical response with the electronic interactions between the macrocycles as well as photoinduced energy or electron transfer processes in these systems.

Tilted "face-to-face" BChl$a$ arrays have been discovered for both LH1(*Rhodospirillum rubrum*)[6] and LH2 (*Rhodopseudomonas acidophila*)[7] complexes (see Figure 1). LH2 contains two BChl$a$ arrays, B800 and B850, and LH1, one array, B875. B800 is a BChl$a$ array of nine monomeric bacteriochlorophylls with a side-by-side arrangement, and B850 is an 18-BChl$a$ array with tilted "face-to-face" configuration[6]. B875 of LH1 has a configuration similar to B850 of LH2[7]. BChl$a$ arrays in B850 and B875 are bound in membrane spanning α-helical peptides in such a way that they are simultaneously J-aggregates in one direction and H-aggregates in another[8]. The configurations of the BChl$a$ arrays as well as their interaction with the protein matrices tune the energies of the different BChl$a$ arrays in such a way that allows a ultrafast energy flow (energetically-downhill) from the outer LH2 to inner LH1 and then to the reaction center (RC) where the initial electron transfer reaction occurs[9].

Moreover, the excited state $<\gamma>$ of BChl$a$ in LH1 and LH2 were also measured. In these cases, the reference state is the excited state S_1 populated by exciting molecules from the ground state S_0. Although whether $<\gamma>$ is still in non-resonant regime is not clear, we have observed dramatic $<\gamma>$ enhancement relative to the ground state for BChl$a$ in LH1, similar to the excitation enhancement observed before in dipenylhexatriene (DPH) solution[10].

2. EXPERIMENTAL

a. Samples

Preparation of BChl$a$ and LH protein samples was described previously[11]. The detergents used in the final solutions for LH1 and LH2 are n-octyl-β-D-glucoside (βOG; 0.8%) and N,N-dimethyldodecylamine-N-oxide (LDAO; 1%), respectively. Both samples were buffered by 10 mM Tris at pH = 7.5. Concentrations of BChl$a$ in the LH2 samples were determined based on the extinction coefficient for BChl$a$ at 850 nm, 184 mM^{-1}cm^{-1}[12], and the molar ratio of BChl$a$ in B800 and in B850[6]. The ϵ_{800} for BChl$a$ in B800 is 240 mM^{-1}cm^{-1} based on our calculation. An ϵ_{880} of 140 mM^{-1}cm^{-1} for BChl$a$ at 875 nm was used to determine the concentration of BChl$a$ in the LH1 sample[13].

b. DFWM and Excited State DFWM Measurements

The laser system for ground state DFWM measurements was described elsewhere[11]. The $\chi^{(3)}$ measurements were carried out with polarization directions of all four laser beams aligned vertically in the laboratory frame. The excited state DFWM mixing experiment was conducted by introducing an excitation laser pulse to the previous DFWM setup. The detail of the experimental setup was described previously[11]. While three 1064 nm pulses (the two pumps and one probe) were overlapped in time and space, the excitation pulse was delayed relative to the 1064 nm pulses. The resulting phase conjugated signal as a function of the delay of the 583 nm excitation pulse was then collected. Details of the femtosecond transient absorption setup were given elsewhere[14,15]. The pump pulse energy was varied to look for the annihilation effect on the ground state recovery kinetics, and the probe wavelengths was set at 855 nm for B850 and at 880 nm for B875, respectively.

The $|\chi^{(3)}|$ reference for the DFWM is CS$_2$ with its $|\chi^{(3)}|$ of 4×10^{-13} esu at 1064 nm[16,17], and n's for the BChl$a$ containing samples were approximated by n of the corresponding solvents (n_{THF}=1.4070 and n_{water}= 1.3330) because of low concentrations of BChl$a$. Using our DFWM setup, only the magnitude, not the phase of the $\chi^{(3)}$ is obtained. The average molecular second hyperpolarizability $<\gamma>$ in an isotropic medium was obtained by,

$$\chi^{(3)} = \chi^{(3)}_{slvt} + 10^{-6} L^4 A <\gamma> C \qquad (1)$$

where *slvt* stands for solvent, A is Avogadro's number and C is the concentration of the solute in mM. Thus, $<\gamma>$ of the solute can be extracted from the slope of the $\chi^{(3)}$ *vs.* C plot.

3. THEORETICAL CALCULATION RESULTS FOR (SiPcO)$_n$ AND THEIR RELEVANCE TO $<\gamma>$ OF BChl$a$ ARRAYS IN LH PROTEINS

In the off-resonant regime, the molecular second order hyperpolarizability tensor $\gamma_{kijh}(\omega_\sigma,\omega_1,\omega_2,\omega_3)$ can be described by the conventional sum-over-states (SOS) expression[18]:

$$\gamma_{kijh}(-\omega_\sigma,\omega_1,\omega_2,\omega_3)=\frac{4}{h^3}I_{-\sigma,1,2,3}[\sum_{\substack{l,m,n \\ m \neq g}}\frac{\mu^k_{gl}\mu^j_{lm}\mu^i_{mn}\mu^h_{ng}}{(\omega_{lg}-\omega_\sigma)(\omega_{mg}-\omega_2-\omega_3)(\omega_{ng}-\omega_3)}-\sum_{m,n}\frac{\mu^k_{gm}\mu^j_{mg}\mu^i_{gn}\mu^h_{ng}}{(\omega_{mg}-\omega_\sigma)(\omega_{mg}+\omega_2)(\omega_{ng}-\omega_3)}] \qquad (2)$$

where μ^c_{ab} represents the cth cartisian component of the transition dipole moment between molecular states a and b and ω_{ab}, the transition frequency for $a \rightarrow b$ transition. The operator $I_{-\sigma,1,2,3}$ denotes that the expression must be averaged over all permutations of the frequencies $-\omega_\sigma$, ω_1, ω_2, and ω_3 with the cartisian components $k, j, i,$ and h permuted simultaneously. The first summation involves those two-photon allowed states, referred to type II terms, and the second term involves four photon volleys between the ground and one-photon allowed states, referred as type I terms. All the excitation are virtual here without significant population depletion of the ground state. The key to obtain a precise γ_{kijh} value is obtain the energy levels and the transition dipoles in the equation (2). Because of the complexity of the structures for the macrocyles, semi-empirical methods with simplified energy levels must be employed. Because the laser frequencies are closer to those virtual transitions with the lowest energies and those transitions are often affected by intermacrocyle π-π interactions, our recent calculations on (SiPcO)$_n$ are based on the Frenkel exciton model for a chain of three level molecules, the ground state |G>, one-photon allowed state |Q> and two-photon allowed state |T>. Using a simplified analysis in the static and near-resonant regimes we identified two mechanisms which lead to enhancements in the dimer or trimer value of $<\gamma>$ over that of the monomer. The first mechanism is a disruption of the balance between type I and type II terms in the sum over states expression for the second hyperpolarizability tensor γ_{kijh} caused by weak intermacrocycle interactions. The second is a near-resonance enhancement of the type II terms due to an intermacrocycle interaction induced shift in the monomer derived two-photon allowed states towards twice the laser photon energy. This analysis is in good agreement with the experimental results. The calculations suggest that the first mechanism is responsible for the 25-fold monomer to dimer enhancement measured in this system and that the additional 4-fold enhancement found in going from the dimer to the trimer is primarily the result of the second mechanism. A complete description of the calculation can be found elsewhere[5].

Although BChl$a$ and SiPcO are different molecular systems and the molecular aggregates in LH1/LH2 and in (SiPcO)$_n$ have different configurations, the results for the latter are still relevant to the former in terms of the effect of the intermacrocycle interactions on $<\gamma>$ enhancement. A more significant enhancement suggests a more altered energy levels from those of the monomer due to stronger intermacrocycle interactions.
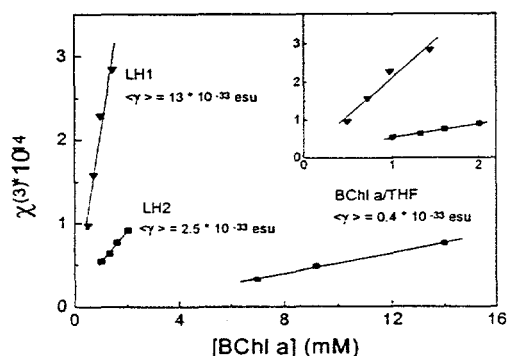

Figure 2. $\chi^{(3)}$ as functions of BChl$a$ concentration in THF, LH1 and LH2. Inset shows the enlarged low concentration region. The $<\gamma>$ values are before correction for sphaeroidene. The $<\gamma>$ value for LH2 is the average value for both B800 and B850 (see text).

4. EXPERIMENTAL RESULTS

a. $<\gamma>$ of BChl a in Different Systems

Figure 2 depicts the concentration dependence of $\chi^{(3)}$ for BChl$a$ in THF, LH1 and LH2. According to Equation (1), $<\gamma>$ of BChl$a$ was extracted from the slopes of the plots, to be 0.4×10^{-33}, 13.3×10^{-33}, and 2.5×10^{-33} esu/BChl$a$ for BChl$a$ in THF, LH1 and LH2, respectively. Based on the measurement conducted under the same conditions, the $<\gamma>$ of BChl$a$ in LH1 and LH2 after the correction for the contribution of sphaeroidene (a molecule with a similar structure as β-carotene) attached to the protein are 13.0×10^{-33} and 2.3×10^{-33} esu/BChl$a$, respectively — 33 and 6 fold increases compared to that in THF. The $<\gamma>$ for the BChl$a$ in B875 of LH1 is 5 times of that in B850 of LH2 for two reasons. First, LH2 contains both B800 and B850 arrays. B800 has a monomeric arrangement for BChl$a$, and the average Mg-Mg distance between two adjacent BChl$a$

is 21.2Å[6], too far for strong electronic interactions. Thus, $<\gamma>$ of BChl$a$ in this array should be similar to that in monomeric BChl$a$ in THF. Consequently, the measured phase conjugated signal from LH2 is predominantly from B850. If we assume that the $<\gamma>$ value for BChl$a$ in B800 of LH2 is the same for BChl$a$ in THF, and subtract it from the total $<\gamma>$ for LH2, the $<\gamma>$ for the BChl$a$ in B850 array would be 3.3×10^{-33} esu/BChl$a$. This $<\gamma>$ value is still four times lower than that of BChl$a$ in B875. Second, the face-to-face interactions between two adjacent BChl$a$ is more favorable in LH1 than in LH2 due to the diameter difference between LH1 and LH2 complexes (see Figure 1). The diameter of the B875 array in LH1 is 92Å[7], which is much larger than 52Å for B850 array in LH2[6]. As 32 and 18 BChl$a$ are arranged symmetrically around B875 and B850 arrays, the average center-to-center distances between two adjacent BChl$a$ are similar, but the angles between two adjacent macrocycle planes are considerably less in the larger array. Therefore, the π-π interaction between two adjacent BChl$a$'s could be stronger in B875 than in B850 resulting in a higher $<\gamma>$.

b. Excited State $<\gamma>$ of BChl$a$ in LH1 and LH2

In the excited state nonresonant DFWM experiment, the pulse used to generate an excited state population will not participate in forming transient gratings, which results in the phase conjugated signal. The effect of the laser excitation is to create a reference state that is the excited state rather than the ground state.

We used a laser pulse at 583 nm to induce a $S_0 \rightarrow S_2$ (Q_x) transition. The initially populated S_2 state decays to S_1 state via internal conversion on a time scale of less than 1 ps[19]. Samples with low BChl$a$ concentrations of 0.14mM (in LH1) and 0.44 mM (in LH2) were used, such that the phase conjugated signals in the absence of a 583 nm pulse were mainly from the solvent (see Figure 3). The signal increases with 583nm excitation are shown in Figure 3. From the fractions of excited BChl$a$ in the samples, $<\gamma>$ values for the S_1 state of BChl$a$ are 7×10^{-31} and 4×10^{-31} esu/BChl$a$ in LH1 and LH2, a factor of 50 and 160 enhancement compared to $<\gamma>$ of the ground state. The origin of the $<\gamma>$ enhancement is not completely clear, because the uncertainly in energy levels of upper excited states as well as the transitions from S_1 state to those states.

Time dependence of the excited state phase conjugated signals for BChl$a$ in LH1 and LH2 is depicted by Figure 4. Because the increase of the excited state $<\gamma>$ is mainly due to changing the reference state from the ground state to one of the excited states, the time dependence of the phase conjugated signals is expected to follow the excited state population decay (affected by energy transfer quenching and singlet-singlet annihilation). We do not intend to establish the excited state dynamics from the phase conjugated signal with the 583 nm excitation here, but merely compare our observation with transient absorption results for the same molecular systems under similar excitation conditions. In Figure 4b, the phase conjugated signal for LH2 has two time constants of 40 ps and 0.9 ns, which correspond well to the transient absorption results with two time constants of 52 ps and 0.948 ns when probing at 855 nm. While the 0.9 ns component corresponds to the singlet excited state decay of BChl$a$ in LH2[20], the faster component could result from singlet-singlet annihilation in aggregates of LH2. The numbers of photons in each laser pulse of 583 nm light in both cases are approaching the annihilation limit with average 1.4 photons/LH2 in DFWM and 1 photons/LH2 in the transient absorption experiments.
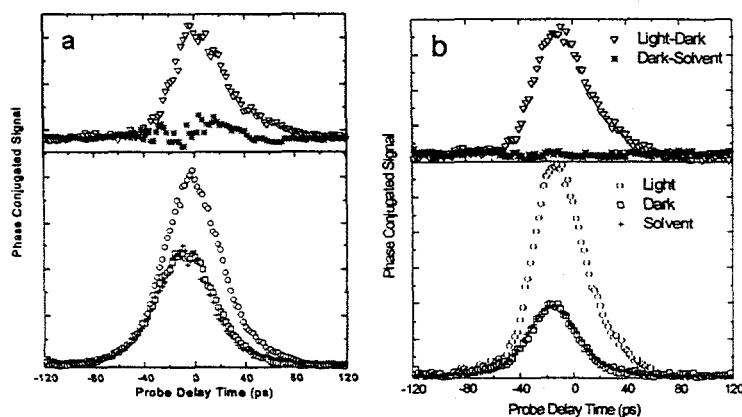
The interpretation of the phase conjugated signal for LH1 is puzzling. At an average of 4 photons/LH1 in each laser pulse, the phase conjugated signal can be fit by one exponential decay with time constant of 350 ps; while at 1 photons/LH1 in each laser pulse, the single exponential decay time constant is 760 ps (with a large uncertainty because of limited time range of the data). In comparison, the time constants of ground state recovery by our transient absorption measurements of LH1 gives a single exponential fit with a time constant of 0.8 ns when

Figure 3. Phase conjugated signals (when 583 nm pulse overlaps with 1064 nm pump pulses) with and without 583 nm excitation as functions of the 1064 nm probe time for (a) 0.14 mM BChl$a$ in LH1 and (b) 0.44 mM BChl$a$ in LH2. The bottom panels display the raw data, and the top panels show the signals from pure solute with and without 583 nm pulses.

exciting with 0.3 photons/LH1 in each laser pulse at 583 nm. Using 3 photons/LH1 in each laser pulse at 583 nm as the excitation source, the transient absorption decay gives an additional 3 ps component due to singlet-singlet excitation annihilation. The 40-50ps component observed in LH2 was absent for LH1. This could be explained by an assumption of energy transfer/singlet-singlet annihilation between LH2 units in a super aggregates, which formed more readily than an aggregate of LH1 in the membrane.

5. DISCUSSIONS

a. Origin of the <γ> Enhancement in LH1 and LH2

Observed in our previous DFWM measurements on μ-oxo SiPcO, <γ> for each macrocyclic unit is enhanced by a factor of 12 in the dimer and a factor of 33 in the trimer compared to that of the monomer[5,6]. This result provides a correlation between the <γ> enhancement and the π-π interactions in the direction that is perpendicular to the macrocycle planes. Comparing <γ> of monomeric BChl$a$ in THF with that in B875 array of LH1 and B850 array of LH2, we observed <γ> enhancement again when BChl$a$ macrocycles are arranged into a circle with tilted "face-to-face" configurations. In cases of BChl$a$ in B875 and B850 arrays, the <γ> for each BChl$a$ is 33 and 8 times of that for monomeric BChl$a$ in THF, respectively.

Because of the differences in monomer structures and in the configuration of the molecular aggregates between μ-oxo SiPc and BChl$a$ in B875 and B850, it is difficult to compare different systems directly and to identify the one that provides a higher <γ> enhancement. At this point, we have not modeled <γ> for a "face-to-face" molecular aggregate as functions of structural parameters; so any conclusion regarding a preferred configuration for an optimized <γ> is premature. Nevertheless, a factor of four increase in <γ> for BChl$a$ in B875 than that in B850 was observed despite similarities in the configurations of protein-bound BChl$a$ arrays. Although, one could relate the progressive increase of the $\chi^{(3)}$ in B800, B850 and B875 by the near resonant one-photon effect that is due to an increasing closeness of the peak frequencies to the laser frequency, this effect alone cannot explain the enhancement factors observed in our experiments. According to the sum-over-state (SOS) expression[18], the enhancement due to this near resonant effect can be estimated to be 1.7 and 2.1 for B850 and B875 compared to B800, much smaller than 8 and 33 observed in the experiment. In our studies of <γ> enhancement in μ-oxo SiPc "face-to-face" oligomers[5], two mechanisms for the <γ> enhancement were proposed: (1) a shift of a two-photon allowed state energy toward to the second harmonic of the laser frequency, and (2) a shift of a charge transfer band toward to laser frequency, both were due to inter-macrocycle π-π interactions when SiPcO oligomers were formed with the "face-to-face" configuration. Our study has indicated that these shifts due to inter-macrocycle interactions can cause a substantial enhancement of <γ> when the monomer <γ> has a well balanced two- and one-photon terms in the SOS expression. If we attribute the <γ> enhancement of BChl$a$ in B850 and B875 similarly to the mechanism (1) or (2), the difference in <γ> values for BChl$a$ in B875 and B850 implies a stronger interaction in the former, resulting from a better "face-to-face" overlap between the macrocycles. Because average center-to-center distances between the adjacent BChl$a$ in B850 and B875 only differ by 0.05Å[6,7], the stronger interaction between macrocycles must come from a pair-wise arrangement in B875. This suggestion agrees with a recent result of hole-burning experiment indicating a stronger interaction between the BChl$a$ in B875 than in B850[21]. It is also worth mentioning that in a recent study of nonlinear absorption in LH2[22], a giant $\chi^{(3)}$ was predicted from strong excitonic coupling within the circular aggregates of BChl$a$. Further theoretical modeling of the $\chi^{(3)}$ enhancement in B875 and B850 has been planned in order to find its origin.
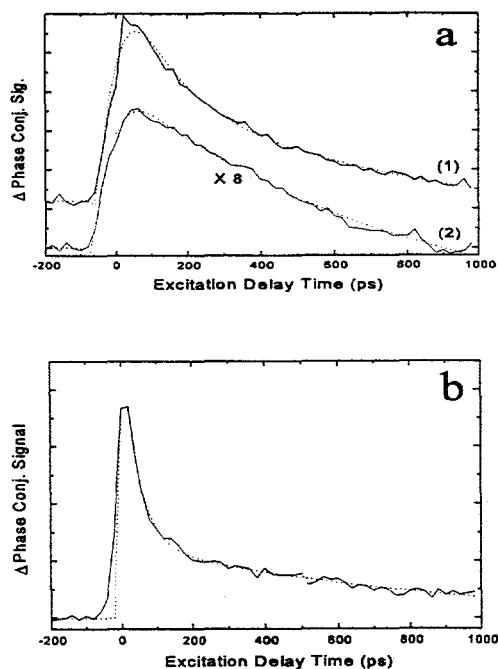

Figure 4. 583 nm excitation delay time dependence of the phase conjugated signal in (a) LH1, with pulse energy of 250μJ (1), and 60μJ (2), and in (b) LH2 with pulse energy of 250μJ. Curve (1) and (2) in (a) were fit by a single exponential decay with a time constant of 350±50ps, 756±14 ps, respectively. The curve in (b) was fit by a sum of two exponentials with coefficients of 0.27 and 0.73 and time constants of 943±79 ps and 44±3 ps.

b. Implication of Excited State $<\gamma>$ Enhancement in Stacked BChla

A significant increase of $<\gamma>$ for BChla in LH1 and LH2 has been observed through our DFWM measurement when an excitation pulse at 583 nm is applied. According to SOS expression of $<\gamma>$ for the DFWM[18], the $<\gamma>$ for one- and two-photon processes are proportional to the products of the transition dipoles from the reference state (normally, the ground state) to the other stationary states and inversely proportional to the products of frequency differences between the laser and transitions from the reference state to the stationary states. Therefore, when an excited state is populated prior to a nonresonant $\chi^{(3)}$ measurement, this state becomes the reference state. During the lifetime of this excited state, the observed enhancement of $<\gamma>$ could result from (1) a decrease in the energy gap between the laser frequency and the transition frequency from the populated excited state to other upper states and (2) increase in the transition dipole moments from the populated excited state to certain other higher states. In particular, for BChla, the enhancement due to S_1 state population may result from increasing contributions of B states which is comparatively unimportant in the ground state $<\gamma>$. However, there is not enough information on the upper state levels and transition dipoles to verify the precise mechanism of the excited state $<\gamma>$ enhancement at this point.

The excited state dynamics of BChla in LH1 and LH2 involve multiple energy transfer and trapping processes have been studied extensively [9,23,24]. However, the details of those processes reflected in the excited state dynamics is not the focus here. Our preliminary results merely show that the phase conjugated signals of excited LH1 and LH2 have been enhanced which correspond to 50 and 160 fold increases in $<\gamma>$ compared to that of the ground state BChla. The ratio of $<\gamma>$ for BChla in LH1 and LH2 is much smaller in excited states than in the ground states, indicating the decrease in the energy gaps between the reference state and the virtual states is the main cause of the enhancement. At 583 nm, the pump laser populates the S_2 state (Q_x excitation) initially, then the S_1 state is populated through a ultrafast internal conversion within 1 ps[19]. The transition frequency from S_1 state to higher excited states could be close to that of photons at 1064 nm, thus, significantly increasing the phase conjugated signal. This observation indicates a potential application in light controlled molecular devices.

6. ACKNOWLEDGMENT

7. REFERENCES

1. P. N. Prasad, D. J. Williams, Introduction to Nonlinear Optical Effects in Molecules and Polymers (Wiley, New York, 1991).
2. D. S. Chemla, J. Zyss, Eds., Nonlinear Optical Properties of Organic Molecules and Crystals, Vol. 1 & 2 (Academic Press, New York, 1987).
3. A. J. Heeger, J. Oreustein, D. R. Ulrich, Eds., Nonlinear Optical Properties of Polymers, Mat. Res. Soc. Symp. Proc., Vol. 109 (MRS: Pittsburgh, 1988).
4. L. X. Chen, B. K. Mandal, B. Bihari, A. K. Sinha, M. Kamath, SPIE Proc. **2527** (1995) 61.
5. E. S. Manas, F. C. Spano, L. X. Chen, J. Chem. Phys., in press.
6. G. McDermott, S. M. Prince, A. A. Freer, A. M. Hawthornthwaite-Lawless, M. Z. Papiz, R. J. Cogdell, N. W. Isaacs, Nature **374** (1995) 517.
7. S. Karrasch, P. A. Bullough, R. Ghosh, The EMBO Journal 14 (1995) 631.
8. A. Freer, S. Prince, K. Sauer, M. Papiz, A. Hawthornthwaite-Lawless, G. McDermott, R. Cogdell, N. Isaacs, Structure 4 (1996) 449.
9. R. van Grondelle, J. P. Dekker, T. Gillbro, V. Sundström, Biochim. Biophys. Acta 1187 (1994)1.
10. (a) J. R. Heflin, D. C. Rodenberger, R. F. Shi, M. Wu, N. Q. Wang, Y. M. Cai, A. F. Garito, Phys. Rev. A **45** (1992) R4233; (b) D. C. Rodenberger, J. R. Heflin, A. F. Garito, *Nature* **359** (1992) 309.
11. L. X. Chen, P. D. Laible, *Chem. Phys. Lett.* **270** (1997) 255.
12. R. K. Clayton, B. J. Clayton, Proc. Natl. Acad. Sci. USA **78** (1981) 5583.

13. R. K. Clayton in Bacterial Photosynthesis, H. Gest, A. San Pietro and L. P. Vernon, eds., (1963) p.495 (Antioch Press, Yellow Springs).

14. S. R. Greenfield, M. Seibert, Govindjee, M. R. Wasielewski, J. Chem. Phys., **B101**, (1997) 2251.

15. S. R. Greenfield, M. R. Wasielewski, Opt. Lett. **259** (1995) 1394.

16. R. W. Hellwarth, Prog. Quant. Electr. **5** (1977) 1.

17. M. J. Moran, C.-Y. She, R. L. Carman, IEEE J. Quant. Electr. **QE-11** (1975) 259.

18. B. J. Orr, J. F. Ward, *Mol. Phys.* **20** (1971) 513.

19. A. O. Ganago, E. P. Parker, P. D. Laible, A. C. Albrecht, T. G. Owens, Laser Physics, **5** (1995) 693.

20. P. Sebban, G. Jolchine, I. Moya, Photochem. Photobiol., **39** (1984) 247.

21. N. R. S. Reddy, H.-M. Wu, R. Jankowiak, R. Picorel, R. J. Cogdell, G. J. Small, Photosynthesis Res., **48** (1996) 277.

22. D. Leupold, J. Stiel, K. Teuchner, F. Nowak, W. Sander, B. Ücker, H. Scheer, Phys. Rev. Lett., **77** (1996) 4675.

23. S. E. Bradforth, R. Jimenez, F. van Mourik, R. van Grondelle, G. R. Fleming, J. Phys. Chem., **99** (1995) 16179.

24. (a) S. Hess, M. Chachisvilis, K. Timpman, M. R. Jones, G. J. S. Fowler, C. N. Hunter, V. Sunström, Proc. Nat. Acta. Sci., USA, **92** (1995) 12333; (b) M. Chachisvilis, T. Pullerits, M. R. Jones, C. N. Hunter, V. Sunström, Chem. Phys. Lett., **224** (1994) 345.